Surface Science 264 (1992) 157–170
North-Holland

surface science

# The NO + $H_2$ reaction on Pt(100): steady state and oscillatory kinetics

M. Slinko [1], T. Fink, T. Löher [2], H.H. Madden, S.J. Lombardo, R. Imbihl and G. Ertl
*Fritz-Haber-Institut der Max-Planck-Gesellschaft, Faradayweg 4–6, D-1000 Berlin 33, Germany*

Received 30 July 1991; accepted for publication 22 October 1991

The reaction of NO + $H_2$ on Pt(100) was studied in the $10^{-6}$ mbar range between 300 and 800 K with mass spectrometry, work-function measurements, and video LEED. Both multiple steady states and kinetic oscillations were found. The principal reaction products were $N_2$, $H_2O$ and $NH_3$, and the activity and selectivity of the reaction were seen to depend on the partial pressure ratio $p_{H_2}/p_{NO}$, on the surface temperature, and on the degree of surface reconstruction. Whereas the 1 × 1 surface of Pt was active for both $N_2$ and $NH_3$ formation, a well-annealed hex phase exhibited a low catalytic activity. The occurrence of defects during the $1 \times 1 \rightleftharpoons$ hex transition was shown to lead to enhanced $N_2$ formation. At low $p_{H_2}/p_{NO}$ ratios, $N_2$ formation was favored while for large $p_{H_2}/p_{NO}$ ratios, $NH_3$ production was enhanced. Kinetic oscillations, as determined from variations in the $N_2$, $H_2O$ and work-function signals, were found between 430 and 445 K.

## 1. Introduction

The catalytic reduction of NO with either CO or $H_2$ is of considerable practical importance due to the pollution effects of NO in air [1]. Moreover, these reactions exhibit interesting dynamical behavior such as multiple steady states and kinetic oscillations. The latter were detected in the NO + CO reaction first on polycrystalline Pt and then on a Pt(100) single-crystal surface where they were studied in the $10^{-7}$ to $10^{-5}$ mbar range [2–5]. The single-crystal study led to the formulation of a mathematical model which reproduced the experimental results quite accurately [5]. The motivation to study the NO + $H_2$ reaction on Pt(100) is that coadsorbed NO and $H_2$ exhibit the same "explosive" product formation upon heating that also has been observed with coadsorbed NO and CO on Pt(100) [6,7]. This similarity suggested that the NO + $H_2$ reaction on Pt(100) would be a suitable candidate for detecting oscillatory behavior.

Sustained kinetic oscillations in the NO + $H_2$ reaction on Pt(100) have been, in fact, detected, as has been shown in a preliminary report [8]. The oscillatory behavior in the NO + $H_2$ reaction is found in that region of parameter space where multiple steady states associated with the $1 \times 1 \rightleftharpoons$ hex phase transition of the Pt(100) surface structure occur. This phase transition influences not only the dissociation probability of NO and hence the catalytic activity, but also the selectivity of the reaction to either $N_2$ and $H_2O$ or $NH_3$ and $H_2O$.

In this paper, a detailed report is presented on the experimental results of the steady state and oscillatory behavior of the NO + $H_2$ reaction on Pt(100). The experimental work is complemented by a numerical study, currently in progress, of a set of coupled differential equations derived from a consideration of the reaction mechanism. A discussion of the oscillation mechanism, which to a great extent relies on the results of the simulations, will be presented in a forthcoming paper together with the results of the simulations.

---

[1] Permanent address: Institute for Chemical Physics, Academy of Sciences of the USSR, Kosygina Street 4, Moscow, 117334, USSR.

[2] Present address: Hahn-Meitner-Institut für Kernforschung Berlin GmbH, Bereich Strahlenchemie, Glieneckerstrasse 100, D-1000 Berlin 39, Germany.

## 2. Experimental

The experiments were performed in a standard UHV chamber evacuated by a combination of a turbomolecular pump (360 ℓ/s), an ion getter pump (180 ℓ/s), and a titanium sublimation pump down to a base pressure of $p < 2 \times 10^{-10}$ mbar. The system was equipped with two mass spectrometers (Balzers OMG111A and Leybold Q-100) with one of them differentially pumped, a piezo-driven Kelvin probe for work-function measurements, and a 4-grid rear-view LEED optics (Omicron) with a video system for quantitative LEED intensity measurements.

The sample was a Pt(100) single crystal of $7 \times 7 \times 1$ mm which had been oriented to $\pm 0.5°$ by Laue diffraction. The crystal was heated resistively through two Ta support wires spot-welded to the upper and lower edges of the sample. The temperature of the crystal was measured by a Ni/NiCr thermocouple and kept constant within $\pm 0.1$ K by a PID controller which also was capable of producing a linear temperature ramp.

The sample surface was cleaned by oxygen treatment at 900 K and $p_{O_2} = 2 \times 10^{-6}$ mbar, and sputtering with $Ar^+$ ions at 760 K followed by annealing to 1050 K. For the experiments, gases with the highest commercial purity available were used (NO (2.8), $H_2$ (5.0), and $D_2$ (2.7)). All partial pressures given in this work have been corrected for differences in the ion gauge sensitivity, $S$, using $S_{H_2}/S_{N_2} = 0.46$ for $H_2$ and $S_{NO}/S_{N_2} = 1.27$ for NO.

## 3. Results

### 3.1. Steady state behavior

The adsorption of the reactants NO and $H_2$ onto a Pt(100) surface has been the subject of a number of quite extensive studies. To summarize

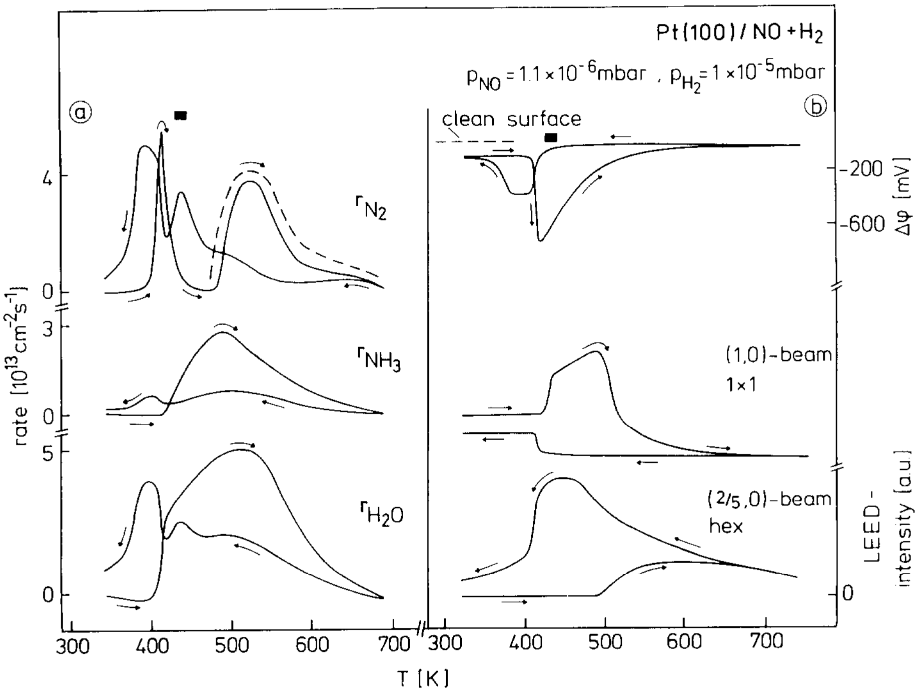

Fig. 1. Hysteresis in the $N_2$, $NH_3$, and $H_2O$ production rates (a) and in the work function and 1 × 1 and hex LEED beam intensities (b) as the temperature is slowly varied in a cycle while constant NO and $H_2O$ partial pressures are maintained. The solid bar indicates the temperature range in which oscillations were observed. The metastable part of the hysteresis is denoted by the dashed line in the $N_2$ production curve. The heating and cooling rate was 0.83 K/s. The LEED measurements here and in all of the following experiments were conducted at normal incidence with a beam energy of 56 eV.

these results, NO adsorbs molecularly at 300 K and causes the hex phase to transform to the $1 \times 1$ phase. When an NO-covered surface is heated above 380 K, the NO dissociates to adsorbed atomic oxygen and atomic nitrogen [7,9–13]. At approximately 400 K, atomic nitrogen recombines to form $N_2$ which desorbs quite rapidly (within ~ 1 s), thereby leaving atomic oxygen on the surface [14]. In contrast to the behavior of NO, hydrogen adsorbs very slowly at room temperature onto the hex phase. Below ~ 250 K, however, substantial hydrogen coverages can be obtained quite rapidly which lead to the removal of the hex reconstruction [15–17]. The most strongly bound adsorption state of hydrogen on Pt(100) desorbs with a peak maximum temperature of 375 K in thermal desorption spectroscopy (TDS) [15,17].

Fig. 1 displays the hysteresis behavior observed when the crystal is slowly heated to 700 K and then cooled in a reaction mixture of NO and $H_2$ at constant $p_{H_2}$ and $p_{NO}$. During the temperature cycle, the rates of production of $N_2$ (mass 28), $H_2O$ (mass 18) and $NH_3$ (mass 17, corrected for the amount of $H_2O$ produced) and the variations in the work function and in the LEED intensities have been followed to measure the degree of reaction and the state of the surface. The reaction rates reported in fig. 1a were calculated by taking into account the effective pumping speed, the crystal dimensions, and the known or measured cracking patterns and ionization probabilities of the species involved. A rather complex hysteresis in all of the measured quantities is observed.

In order to account for the features in fig. 1, it is useful to consider the following set of elementary steps:

$$NO + * \rightleftharpoons NO_{ad}, \tag{R1}$$

$$H_2 + 2* \rightleftharpoons 2H_{ad}, \tag{R2}$$

$$NO_{ad} + * \rightarrow N_{ad} + O_{ad}, \tag{R3}$$

$$2N_{ad} \rightarrow N_2 + 2*, \tag{R4}$$

$$O_{ad} + 2H_{ad} \rightarrow H_2O + 3*, \tag{R5}$$

$$N_{ad} + 3H_{ad} \rightleftharpoons NH_{3,ad} + 3*, \tag{R6}$$

$$NH_{3,ad} \rightarrow NH_3 + *, \tag{R7}$$

where * denotes a free adsorption site.

The primary reaction products are $N_2$ (R4), $H_2O$ (R5) and $NH_3$ (R6). All reaction intermediates in the formation of $H_2O$ and $NH_3$ have been neglected, and it has been assumed that $H_2O$ desorbs practically instantaneously after its formation. A key step in the mechanism is the dissociation of NO (R3), since this step is necessary in order to form the atomic nitrogen and oxygen needed for the subsequent formation of $N_2$, $H_2O$ and $NH_3$. As demonstrated in previous studies, $N_2O$ may also appear as a reaction product in the NO + $H_2$ reaction on a Pt surface [18]. It amounts, however, to less than 10% of the main products and therefore is not included here.

In the light of the above mechanism, the principal features in the hysteresis in fig. 1 can be readily understood. As the crystal is heated from 350 to 400 K, a high coverage of NO stabilizes the $1 \times 1$ surface. The reaction rate is low, since dissociation of NO requires vacant sites and therefore cannot proceed at high adsorbate coverages [7]. Above 400 K, the desorption of NO and $H_2$ creates vacant sites and the reaction accelerates rapidly as evidenced by the sharp rise of the $N_2$ and $H_2O$ production rates. When a higher heating rate of 1 K/s is used instead of 0.83 K/s used here, the maximum in the reaction rate at 420 K transforms into a spike-like feature. This narrow signal is reminiscent of the so-called "surface explosion" of coadsorbed NO and $H_2$, which apparently also takes place under the reaction conditions used here. If one writes down the stoichiometric equations for $NH_3$ and $N_2$ formation in the following way:

$$NO + H_2 \rightarrow \tfrac{1}{2}N_2 + H_2O,$$

$$NO + 2.5H_2 \rightarrow NH_3 + H_2O,$$

one realizes that the $H_2O$ production rate reflects the overall catalyst activity. This is qualitatively what is seen in fig. 1a.

In order to understand the appearance of the remaining features in fig. 1a, it is necessary to take into account the state of the surface as monitored by the work function and the LEED intensities. The $\Delta\phi$-trace in fig. 1b shows that the work function in the course of the hysteresis always remains below the level of the clean hex surface. The most prominent feature in the $\Delta\phi$ trace in fig. 1b is the minimum in the work function of ~ 700 mV below the level of the clean hex phase. Both $NH_3$ and $H_2O$ adsorbed on Pt surfaces are known to lead to large decreases of the work function of $-3$ and $-1$ V, respectively [19,20]. In contrast to these large work-function changes, molecularly adsorbed NO only causes a maximum $\Delta\phi$ change of $-50$ mV [7], while adsorbed hydrogen at temperatures above 300 K leads to a maximum $\Delta\phi$ increase of ~ 100 mV (see fig. 4). Thus, the reaction products $NH_3$ and $H_2O$ and their intermediates are the only candidates whose presence could account for such a strong $\Delta\phi$ decrease. Since TDS studies [21,22] reveal that $H_2O$ desorbs from Pt(100) at $T < 200$ K, while $NH_3$ exhibits a strongly bound adsorption state which desorbs between 300 and 500 K, the $\Delta\phi$-drop in fig. 1b can be assigned to adsorbed $NH_3$.

We cannot exclude the possibility that NH or $NH_2$ species exist on the surface and therefore the assignment to molecularly adsorbed $NH_3$ is only tentative. This assignment is substantiated, however, by the proximity of the $\Delta\phi$ minimum with the peak at $T = 490$ K in the $NH_3$ hysteresis in fig. 1a. The differences in peak location stems from the fact that the decrease in $\Delta\phi$ reflects the formation of $NH_3$ on the surface whereas the mass spectrometer measures the enhanced $NH_3$ desorption rate as the temperature is increased. If one assumes an average dipole moment $\mu_s = 2.0$ D for adsorbed $NH_3$, an $NH_3$ coverage $\theta_{NH_3} \approx 0.06$ can be estimated at the $\Delta\phi$ minimum [19].

From previous investigations, it is known that only the 1 × 1 phase is active in NO dissociation while the hex phase exhibits a rather low efficiency for NO dissociation [6,7,9]. One would therefore expect that the overall catalytic activity in the NO + $H_2$ reaction, as monitored by $H_2O$ formation, would decrease upon heating as the 1 × 1 phase transforms into the less active hex phase. Upon comparison of the LEED intensity curves in fig. 1b with the $H_2O$ hysteresis in fig. 1a, it can be seen that the decrease in the overall catalytic activity above 500 K indeed coincides with the formation of the hex phase. The hysteresis in the surface structure, which is monitored by the intensity of the hex beam in fig. 1b, is very similar to that observed when the crystal is heated and cooled in pure NO [7]. Apparently, an adsorption/desorption equilibrium of NO controls the phase transition in both directions with only a small influence of $H_2$ in the gas atmosphere.

The occurrence of the phase transition has a pronounced effect on the relative amounts of $N_2$ and $NH_3$ produced. Referring again to figs. 1a and 1b, it can be seen that as the temperature is increased above 450 K, the increase in production of $N_2$ coincides with the formation of the hex phase whereas $NH_3$ production is seen to decrease. Upon further heating, the catalyst activity approaches zero for all three reaction products as a consequence of negligible NO dissociation on the hex phase. As the sample is cooled in the $NO/H_2$ atmosphere, the hex phase persists until 420 K at which point the hex → 1 × 1 phase transition occurs. In the temperature region immediately after the phase transition, the catalyst is seen to produce predominantly $N_2$ whereas at temperatures well below the phase transition, the catalyst returns to its adsorbate-covered state with negligible activity.

The comparison between figs. 1a and 1b demonstrates that the 1 × 1 → hex phase transition modifies the selectivity of the reaction from preferential $NH_3$ production on the 1 × 1 phase to preferential $N_2$ formation on the hex phase. The high level of $N_2$ production in the latter case is not due to the hex phase itself, but can be attributed to the presence of structural defects. Experimental evidence for the existence of structural defects is provided by the following. When the previous experiment is repeated with a maximum temperature of 550 K instead of 700 K, one obtains the hysteresis curves which are displayed in fig. 2. The main difference in the hysteresis behavior with respect to the previous experiment is that during the cooling branch, the hex phase is now associated with a rather high level of $N_2$ production as compared to the lower level of $N_2$ production in fig. 1a.

Upon comparison of figs. 1 and 2, it can be seen that although the surface reconstructs to the hex phase in both cases, it exhibits a very different level in catalytic activity depending on the maximum temperature used in the heating cycle. The LEED measurements in fig. 1b demonstrate that annealing to 750 K improves the maximum level of the hex intensity as compared with the LEED measurements in fig. 2b. Evidently, heating the sample up to 550 K is not sufficient to produce a well-ordered hex phase. The difference in catalytic activity can thus be ascribed to structural defects on the hex phase, which from previous investigations are known to facilitate the dissociation of NO [5,23,24]. These structural defects inevitably form during the 1 × 1 → hex phase transition, since the substrate phases differ by ~ 20% in their density of surface atoms.

The time-dependence of the concentration of structural defects has been monitored in the following way. A temperature hysteresis was conducted in a NO + $H_2$ mixture and the heating schedule was stopped and held at $T = 550$ K. It was then observed that the $N_2$ production rate does not remain stationary but returns within minutes from the upper rate branch to the lower rate branch. The hysteresis observed at this temperature is therefore not a true hysteresis but rather is caused by kinetic effects, e.g., by the presence of structural defects which require some time for their annealing. Of the two rate branches depicted in fig. 1a, the metastable part is marked by a dashed line in the $r_{N_2}$ trace. The rest represents in fact a true hysteresis as has been verified by stopping the heating schedule at various points of the temperature cycle and observing a constant rate.

The influence of the $H_2$ partial pressure on the activity and selectivity of the reaction on the two surface phases has also been examined. As depicted in fig. 3, the partial pressures of the products $N_2$, $H_2O$ and $NH_3$ were followed by varying $p_{H_2}$ at $p_{NO} = 1.1 \times 10^{-6}$ mbar. The full line represents the rate curves for a surface heated to $T = 445$ K whereas the dashed curves were recorded after the sample had been first heated in an NO/$H_2$ mixture to 550 K and then cooled to 445 K. The full line therefore represents the reaction taking place on a 1 × 1 surface, while the dashed line displays the reaction kinetics occur-

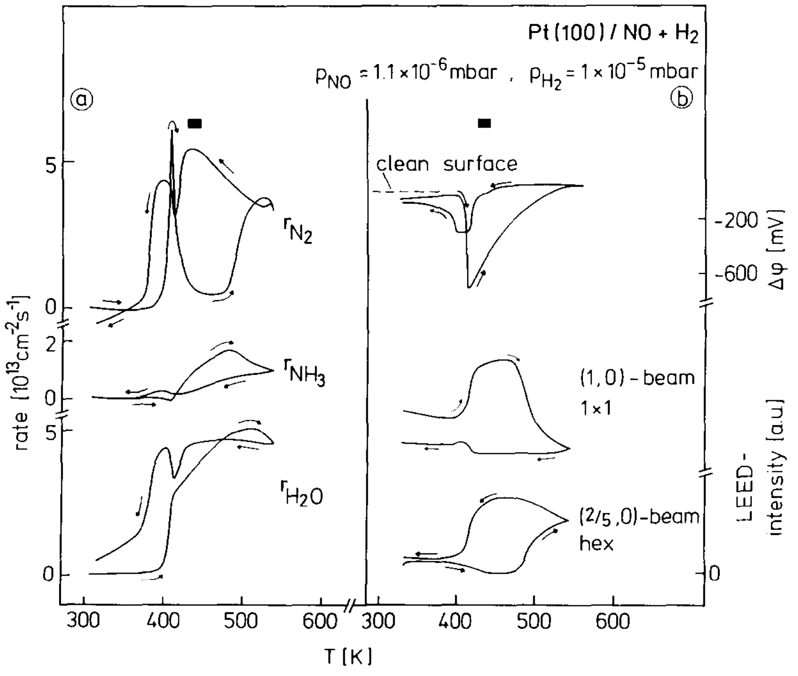

Fig. 2. Same as in fig. 1 but in this case the maximum temperature in the hysteresis is 550 K instead of 700 K as in fig. 1.

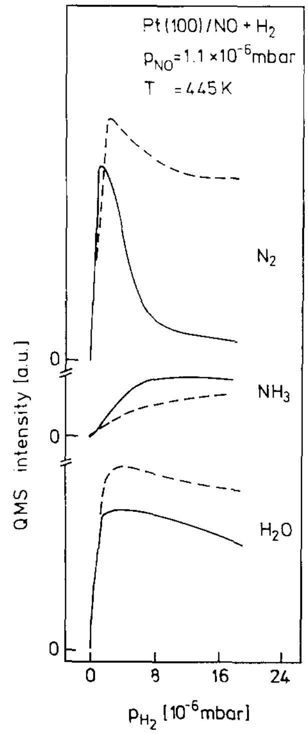

Fig. 3. Dependence of the $N_2$, $NH_3$, and $H_2O$ production rates on the $H_2$ partial pressure and on the surface structure. The solid line indicates the intensities measured for a surface heated in an $NO/H_2$ to 445 K thereby producing a 1×1 surface whereas the dashed line shows the intensities for a surface heated to 550 K and then cooled to 445 K in an $NO/H_2$ mixture thus producing a partially reconstructed surface.

ring on a hex surface with a large amount of defects, i.e., on a partially reconstructed surface. First, one can clearly distinguish between two different regions in the kinetics of the reaction. At low $p_{H_2}$, the production of $H_2O$ and $N_2$ rises extremely steeply with increasing $p_{H_2}$, while $NH_3$ production remains low. As $p_{H_2}$ is further increased, the production of $N_2$ goes through a maximum, while the $NH_3$ production rate continues to increase. These results demonstrate that $NH_3$ formation is the preferred reaction product when $p_{H_2}/p_{NO}$ is large, whereas $N_2$ production predominates when $p_{H_2}/p_{NO}$ is small. The role of the structural sensitivity of the reaction is also apparent in fig. 3 when one compares the rates of $N_2$ and $NH_3$ production on the 1 × 1 surface (full curve) and on the hex surface with defects (dashed curve). On the hex surface with defects, the $N_2$ production rate remains high even when $H_2$ is in excess, whereas $N_2$ production decreases quite strongly on the 1 × 1 surface when hydrogen is in excess.

The influence of surface structure on the selectivity of the reaction can be understood quite simply if one considers the different adsorption properties of hydrogen on the 1 × 1 and hex phases. Fig. 4 displays the hysteresis in $\Delta\phi$ and in the LEED intensities which are observed when a Pt(100) surface is slowly heated and cooled in an $H_2$ atmosphere at constant $p_{H_2}$. The hysteresis in the hydrogen coverage, which is monitored here by $\Delta\phi$, is associated with a hysteresis in the surface structure caused by the hydrogen-induced lifting of the hex reconstruction. Starting at high temperature, which corresponds to the surface in the hex state with a negligible hydrogen coverage, one observes little change in $\Delta\phi$ upon cooling. At temperatures below 250 K, however, the adsorption of hydrogen leads to a hydrogen-covered

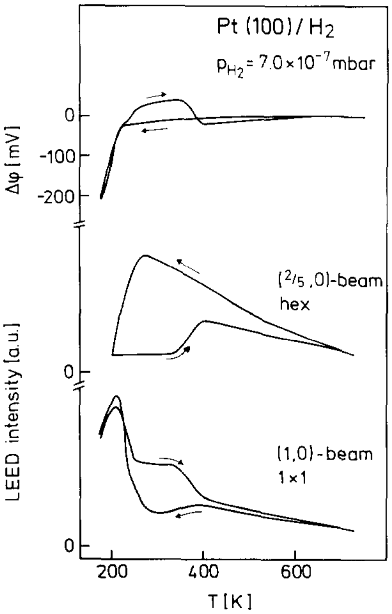

Fig. 4. Hysteresis in the adsorption/desorption equilibrium of $H_2$ on Pt(100). The work function and the 1×1 and hex LEED beam intensities were recorded as the temperature is slowly varied in a cycle while maintaining a constant $H_2$ pressure.

$1 \times 1$ phase and heating above 400 K is necessary in order to restore the clean hex phase. At this temperature, almost all of the hydrogen from the $1 \times 1$ phase is desorbed.

The hysteresis observed here with $H_2$ on Pt(100) is completely analogous to the systems Pt(100)/CO, Pt(100)/NO and Pt(100)/$O_2$ in which the adsorbates also lead to a lifting of the hex reconstruction [7,25,26]. The origin of the hysteresis can very likely be explained in the same way as has been proposed for Pt(100)/CO, where the lower adsorption energy of CO on the hex phase as compared to the $1 \times 1$ phase has been shown to be the main thermodynamical driving force [25]. Some details in the $\Delta\phi$ behavior seem to be noteworthy. Hydrogen adsorption causes a lowering of $\Delta\phi$ below 300 K, but the high-temperature adsorption state which remains on the $1 \times 1$ surface after heating beyond 300 K gives rise to an increase in the work function by ~ 100 mV. Apparently, different adsorption states with opposite dipole moments occur in the system Pt(100)/$H_2$ [17]. The state which is relevant under the conditions here is clearly the high temperature state associated with an increase of the work function.

The selectivity behavior of the reaction to either $N_2$ or $NH_3$ which has been observed in figs. 1–3 for the $1 \times 1$ phase and for the well-annealed hex phase can be compactly summarized by taking into account the availability of hydrogen on the surface. When the hydrogen coverage on the surface is high, $NH_3$ formation is enhanced whereas in the absence of hydrogen, only $N_2$ is formed. The influence of the surface structure on the $N_2$/$NH_3$ product ratio can be explained in light of the different adsorption properties of hydrogen on the two surface phases. Since the $1 \times 1$ surface adsorbs hydrogen much more readily than the hex phase, $NH_3$ formation occurs on this surface, whereas on the hex phase the limited availability of hydrogen makes $NH_3$ production less favorable.

### 3.2. Kinetic oscillations

Kinetic oscillations in the NO + $H_2$ reaction on Pt(100) have been observed by heating the sample to 550 K in an NO/$H_2$ atmosphere followed by slowly decreasing the temperature. The values of the $N_2$ production rate and work function during this type of heating schedule are shown in fig. 5. In a rather narrow temperature region between 430 to 445 K width, oscillations in the reaction rate were observed. As indicated by the solid bars in figs. 1, 2 and 5, the temperature region in which oscillations have been obtained coincides with the lifting of the hex reconstruction and with the beginning of a steep drop in $\Delta\phi$ monitoring the formation of a stationary $NH_3$ coverage on the surface.

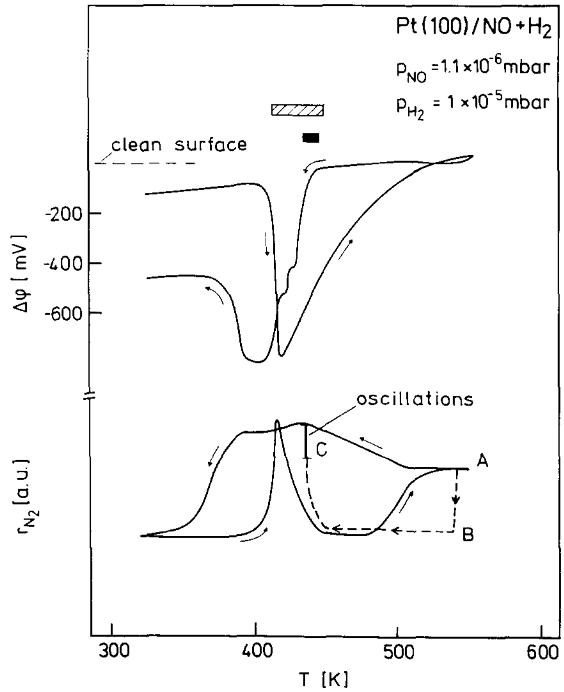

Fig. 5. Hysteresis in the work function and in the $N_2$ intensity during the temperature cycles used for establishing kinetic oscillations. The solid bar indicates the temperature range in which oscillations were observed. Oscillations were found on the cooling branch of the hysteresis when the sample was cooled sufficiently rapidly so that the reaction remained on the metastable upper branch of the $N_2$ production rate (path AC) or when the cooling was sufficiently slow so that the reaction proceeded along the lower rate branch of the kinetics (path ABC, i.e., along the dotted line). The vertical bar C denotes the maximum amplitude of the oscillations. The shaded bar denotes the region where the reaction exhibits a high temperature sensitivity (see fig. 9).

The appearance of kinetic oscillations at a constant temperature is a slow process. As depicted in fig. 6, an induction period of 20 min exists before stable, large amplitude oscillations develop. The length of the induction period depends on the cooling rate from the maximum temperature in the hysteresis to the temperature at which oscillations occur. For a cooling rate of 0.11 K/s, the induction period may last only two to three minutes, but when the sample is cooled more rapidly at 0.5 K/s, the induction period increases to roughly 30 min. A continuous slow downward shift in $\Delta\phi$ of ~ 100 mV per hour is observed, even after seemingly stable large-amplitude oscillations in the $N_2$ production rate are achieved. It may well be that this shift is just due to a slow increase in the $NH_3$ coverage as a consequence of an enhanced $NH_3$ background pressure during the course of an experiment.

In all experiments, kinetic oscillations were only found to occur on the cooling branch of the hysteresis. In one type of experiment, the sample was first heated to 550 K and then cooled. For this type of temperature cycle, the $N_2$ intensity upon cooling followed the metastable high rate branch as indicated by path AC in fig. 5. This is, however, not the only pathway which leads to kinetic oscillations. In a second type of experiment, the temperature was first heated to 550 K and then held at this temperature to anneal defects before cooling. The $N_2$ intensity for this type of heating schedule followed the trajectory along the low rate branch as indicated by the dashed line in fig. 5. The properties of the oscillations which are obtained in this manner exhibit no notable differences to those of the previous procedure. Apparently, the initial level of surface defects on the hex phase has no detectable influence on the oscillatory properties of the system.

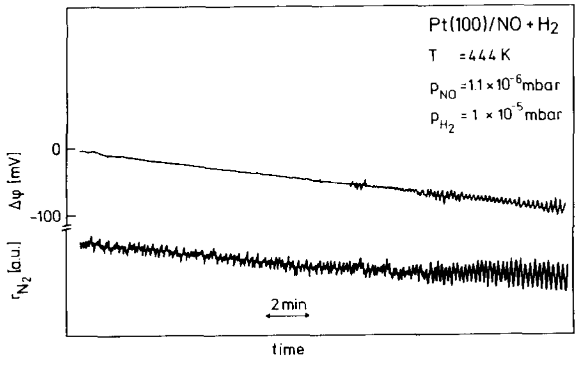

Fig. 6. Temporal variations in the work function and $N_2$ intensity after the temperature was lowered to 444 K. Oscillations are seen to occur after an induction period.

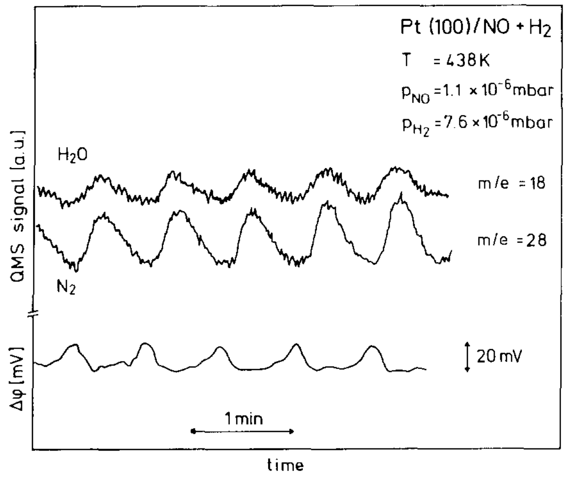

Fig. 7. Temporal variations in the work function and in the $H_2O$ and $N_2$ production rates during oscillations. A constant phase relationship between the signals is seen.

The temporal variation of $\Delta\phi$ and of the reaction products $N_2$ and $H_2O$ during kinetic oscillations are shown in fig. 7. Both $N_2$ and $H_2O$ are seen to oscillate in phase whereas the $\Delta\phi$ signal is shifted by 180° relative to the $N_2$ and $H_2O$ signals. The variations in $\Delta\phi$ can be attributed to either changes in atomic oxygen coverage or to changes in $NH_3$ coverage. The observation that the oscillations in $\Delta\phi$ always take place with the average value being below the $\Delta\phi$ level of the clean hex phase indicates that the periodic variations occur in the presence of a finite $NH_3$ coverage. From the changes in $\Delta\phi$, it can be estimated that the changes in $NH_3$ coverage during the course of oscillations are less than 1% of a monolayer and thus the variations in $r_{NH_3}$ in the gas phase may well be below the detection limit.

The fact that kinetic oscillations in the NO + $H_2$ reaction occur only under conditions of a partially reconstructed Pt(100) surface might indicate that the $1 \times 1 \rightleftharpoons$ hex phase transition plays a role in the mechanism of oscillations as has been shown for Pt(100)/CO + $O_2$ [27]. In order to determine if this were the case, in situ LEED experiments were conducted. In none of these experiments were the oscillations in the reaction rate accompanied by periodic variations of the hex or 1 × 1 intensities. A typical example of such an experiment is displayed in fig. 8. Neither the regular oscillations nor the large amplitude changes in $r_{N_2}$ initiated by small temperature decreases caused any notable effect on the intensities of the integral or fractional order beams. Even though low beam currents of 0.10 $\mu$A have been used in the experiments, it might be possible that beam damaging effects prevent the detection of oscillatory structural changes. This could happen if the electron beam suppresses locally the oscillations, while they continue in the surface area which is not hit by the electron beam.

A characteristic of the reaction in the vicinity of the region for oscillations is the extreme sensitivity of the reaction rate to small temperature changes. As shown in fig. 9, a temperature decrease of 4 K causes large excursions in the $N_2$ production rate and in the value of $\Delta\phi$. Interestingly, the level of $N_2$ production seen in fig. 9 is restored soon after the temperature jump whereas $\Delta\phi$ attains a lower value. The temperature range over which this temperature sensitivity has been observed is indicated by the shaded bar in fig. 5.

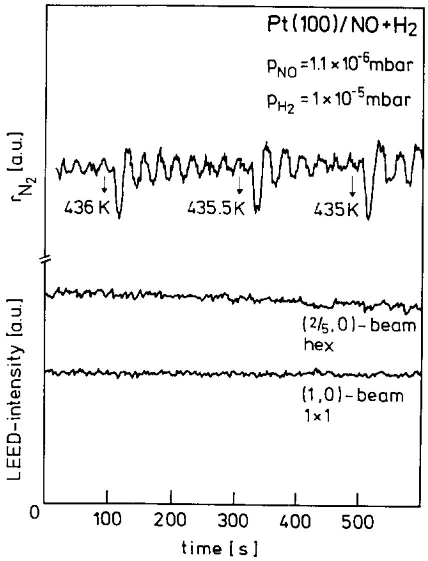

Fig. 8. Temporal variations in the $N_2$ production rate and in the 1×1 and hex LEED beam intensities during oscillations. The arrows indicate the times at which the temperature was decreased by 0.5 K.

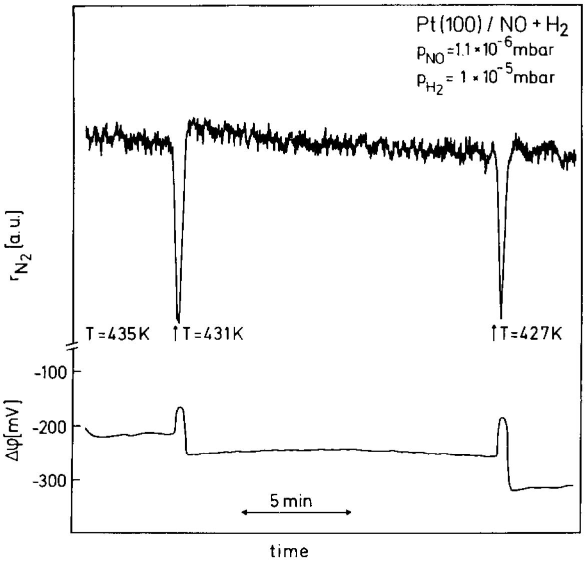

Fig. 9. Effect of small temperature changes on the $N_2$ production rate and on the work function in the region where the reaction responds extremely sensitively to temperature variations. This temperature range is indicated by the shaded bar in fig. 5.

A tentative explanation for this sensitivity is the following. From fig. 5, one notes that in the temperature region where oscillations are observed, high levels of $N_2$ production occur. In this same temperature region, the occurrence of the hex → 1 × 1 phase transition is not seen to noticeably change the amount of $N_2$ produced. If the primary effect of the small decrease in temperature is to further the NO-induced lifting of the hex reconstruction, the change in the relative amounts of substrate phases might not be associated with any notable difference in $r_{N_2}$. The only difference will be that the increase in the 1 × 1 area enhances $NH_3$ production and thus causes a lower $\Delta\phi$ level, which is exactly what is observed in fig. 9.

In fig. 10 is displayed a series of oscillation patterns for selected values of the temperature. Near the upper $T$ boundary, oscillations have a

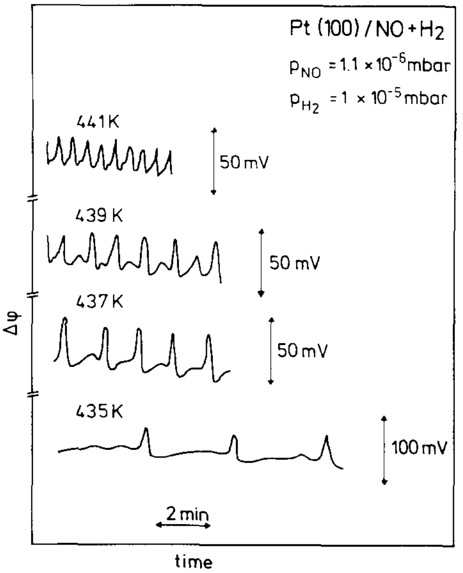

Fig. 10. Oscillation wave forms in the work-function change for selected temperatures within the existence region for oscillations.

small amplitude and a period of ~ 5 to 20 s. For intermediate temperatures, both the amplitude and the period of the oscillations becomes larger. Towards the lower $T$ boundary, the period of the oscillations becomes very large, while the amplitude remains constant. This behavior at lower temperature is characteristic of a so-called homoclinic bifurcation in which the period goes towards infinity at the bifurcation whereas the amplitude of the oscillations collapses in a discontinuous transition beyond the bifurcation point.

The magnitude of the oscillation period at different temperatures is depicted in fig. 11 for two different values of $p_{H_2}$ with $p_{NO}$ being kept the same. One notes that the existence range for oscillations is shifted 10 K towards higher temperature when $p_{H_2}$ is increased by a factor of 3. The same diagram shows that an increase in $p_{H_2}$ at constant temperature and constant $p_{NO}$ leads to longer oscillation periods. The plot in fig. 11 also shows that large changes in $p_{H_2}$ do not significantly alter the way in which the oscillation period depends on temperature. The oscillations were also found to be stable over a wide range of hydrogen pressures. After having been first established at the conditions of $p_{NO} = 1.1 \times 10^{-6}$ mbar, $p_{H_2} = 1 \times 10^{-5}$ mbar and $T = 440$ K, oscillations were stable for changes in the hydrogen pressure between $4 \times 10^{-6}$ and $3 \times 10^{-5}$ mbar, i.e., for $p_{H_2}/p_{NO}$ ratios between 4:1 and 30:1.

The temperature dependence of the oscillation amplitude of $\Delta\phi$ is shown in fig. 12 for different values of $p_{H_2}$. As seen in fig. 12, the oscillations start with a small amplitude in $\Delta\phi$ at the high $T$ boundary and then grow continuously with decreasing temperature until the oscillations disappear in a sharp transition at the low $T$ boundary. This kind of behavior is consistent with a Hopf bifurcation at the high $T$ boundary and a homoclinic bifurcation at the low $T$ boundary. For the lowest $p_{H_2}/p_{NO}$ value used in this study, the amplitude of $\Delta\phi$ is quite small. In a rather broad range of intermediate $p_{H_2}/p_{NO}$ values, the maximum amplitude of the $\Delta\phi$-oscillations is practically independent of $p_{H_2}$ as shown in fig. 12 for $p_{H_2} = 5.6 \times 10^{-6}$ mbar and $p_{H_2} = 1.0 \times 10^{-5}$ mbar.

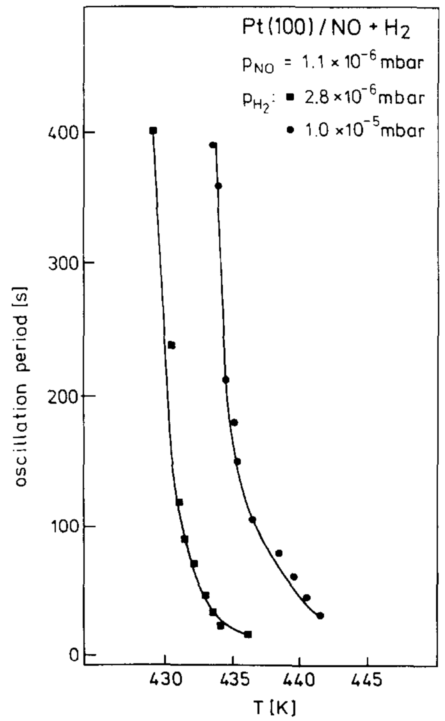

Fig. 11. Temperature dependence of the oscillation period for two $H_2$ partial pressures.

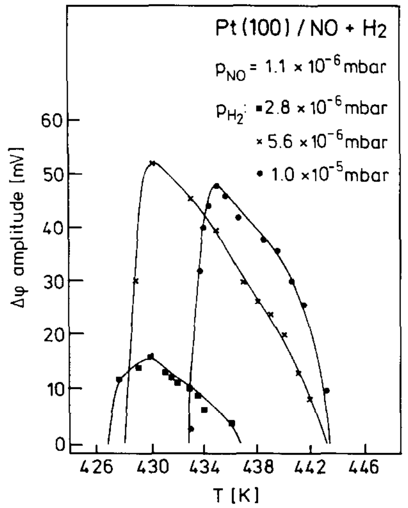

Fig. 12. Temperature dependence of the oscillation amplitude as measured via the work-function change for several $H_2$ partial pressures.

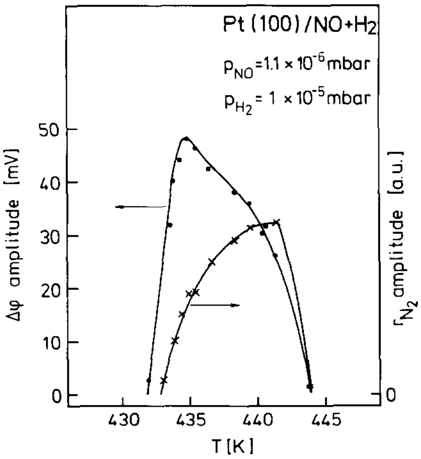

Fig. 13. Differences in the temperature dependence of the oscillation amplitude as measured through the work-function change and the $N_2$ production rate.

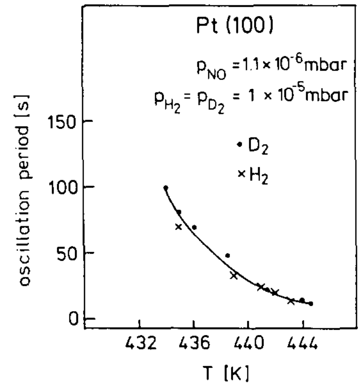

Fig. 14. Comparison of the temperature dependence of the oscillation period for NO/$H_2$ and NO/$D_2$ mixtures demonstrating the absence of an isotope effect.

An interesting relationship is obtained by comparing the amplitudes of the oscillations of $\Delta\phi$ and $r_{N_2}$ at different temperatures. As can be seen from fig. 13, the temperature dependence of the amplitudes for $\Delta\phi$ and $N_2$ do not vary in the same way. Large oscillations in $N_2$ production are found at the upper $T$ boundary, while large amplitudes in the $\Delta\phi$ oscillations are located at the lower $T$ boundary. This relationship suggests that the selectivity for the reaction changes as the temperature is lowered from preferential $N_2$ production at high temperature to a more enhanced $NH_3$ production at lower temperature. The competition between the two different channels might, in fact, be an essential part of the oscillation mechanism itself.

Experiments were also conducted in which $D_2$ was used in the reaction mixture in place of $H_2$. The results of these experiments, which are displayed in fig. 14, show that neither the period of the oscillations nor the existence range is influenced by any H/D isotopic effect. Such an effect might be expected if either the surface diffusion of hydrogen or the addition of atomic hydrogen in forming water and ammonia would play an important role in the rate-determining step of the kinetic oscillations [28].

## 4. Discussion

To date, only a few studies have reported on the NO + $H_2$ reaction on Pt surfaces [1,18,29–31]. The principal observations made in these studies with respect to the parameter dependence of the different production rates for $N_2$, $H_2O$ and $NH_3$ are all consistent with the results obtained here. Studies that have been performed at low pressure ($< 10^{-6}$ mbar) with Pt(111) and polycrystalline Pt have demonstrated that $N_2$ is the main reaction product at low $p_{H_2}$, while $NH_3$ is preferentially formed in excess $H_2$ [18,29].

In addition to the $H_2$ pressure dependence, the surface structure is also seen to influence the selectivity of the reaction. Both $N_2$ and $NH_3$ are formed on the 1 × 1 phase, whereas primarily only $N_2$ is formed on the hex phase. This structural dependence is closely related to the hydrogen concentration discussed above, since the 1 × 1 phase adsorbs hydrogen much more rapidly than does the hex phase.

Although the oscillations in the NO + $H_2$ reaction on Pt(100) appear to involve a rather complex mechanism, a comparison with the oscillations in the NO + CO reaction on the same surface reveals a number of close similarities [4,5]. In both systems, the oscillations occur in the $10^{-6}$ mbar total pressure range between 400 and 450 K and the existence ranges are 10–15 K wide. This is the same temperature region in which the "surface explosion" has also been seen to occur. This phenomenon is clearly the most remarkable property both systems have in common. In the case of NO + CO, it was demonstrated by a mathematical model that the "surface explosion" is, in fact, an essential part of the oscillation mechanism for the NO + CO reaction on Pt(100) [5]. Aside from these more general considerations, kinetic oscillations exist in both cases on the cooling branch of the rate hysteresis and they cannot be initiated at constant temperature by varying the partial pressures. The oscillations in both cases were seen to exhibit a rather high sensitivity to small temperature changes and a relatively small sensitivity to partial pressure variations.

There exist, however, a number of pronounced differences in the oscillatory behavior of the two systems. The most prominent one is clearly the fact that the NO + $H_2$ reaction exhibits sustained oscillations whereas the amplitude of the oscillations in the NO + CO reaction always decay after an initial excitation. The damping effect observed in the NO + CO oscillations was not attributed to a particular mechanistic step, but rather to an insufficient synchronization of the different local oscillators on the surface [5]. Spatially resolved measurements with a photoemission electron microscope (PEEM) confirmed this interpretation for the NO + CO reaction, since they demonstrated that after an initial excitation, a transition from a regular to a chaotic spatiotemporal pattern occurs [32]. The regular spatiotemporal pattern reflects a system oscillating synchronously on a large length scale whereas the small-scale chaotic patterns are evidence of local oscillators out of phase whose integrated effects exhibit no oscillations. Since the NO + $H_2$ reaction exhibits sustained oscillations, the coupling of the local oscillators in this system must be much stronger than for the NO + CO reaction. Modulation experiments in which the NO pressure was sinusoidally varied showed that amplitude variations of 3% of the NO pressure lead to harmonic entrainment. Thus, gas-phase coupling is likely the source of synchronicity in the NO + $H_2$ system and causes sustained oscillations. To verify this, spatially resolved surface measurements with PEEM are planned for the near future.

The close similarities in the oscillatory behavior between the NO + CO and the NO + $H_2$ reactions suggest that the oscillation mechanism might be the same in both systems. If this is the case, one should also observe oscillations in the NO + $H_2$ reaction on a surface which is entirely in a 1 × 1 state, since the oscillation mechanism for the NO + CO reaction did not involve the 1 × 1 $\rightleftharpoons$ hex phase transition. The absence of oscillations in the NO + $H_2$ system on an entirely 1 × 1 surface can be explained if one examines the chemical differences between the two reaction systems more closely. While the products $CO_2$ and $N_2$ in the CO + NO reaction are almost immediately released into the gas phase after formation and therefore cannot block adsorption sites, the $NH_3$ which is produced in the NO + $H_2$ reaction desorbs relatively slowly and may accumulate on the surface. Therefore it appears plausible that kinetic oscillations in the NO + $H_2$ reaction require a largely reconstructed surface simply because a pure 1 × 1 substrate would lead to a poisoning of the surface reaction due to its high $NH_3$ production rate.

Although all of the details of the oscillation mechanism in the NO + $H_2$ system are not known, the experimental evidence available clearly suggests that the essential step is the same as for the NO + CO reaction, namely, the autocatalytic behavior of the surface reaction which leads to the occurrence of a so-called "surface explosion". The step in the reaction which causes the "surface explosion" is the dissociation of NO which requires a vacant site in order to proceed. Starting with a high adsorbate coverage, the reaction accelerates very rapidly once vacant sites are created:

R3 + 0.5R4 + R5:

$$NO_{ad} + 2H_{ad} + * \rightarrow H_2O + \tfrac{1}{2}N_2 + 4* .$$

The bare surface created by the "surface explosion" will, under reaction conditions, soon be covered with adsorbate again. In this way, a periodic sequence of "surface explosions" and reformation of a mixed adsorbate layer may constitute the oscillatory mechanism.

The formation of $NH_3$ in the NO + $H_2$ reaction brings an additional complication into the discussion of the oscillation mechanism. NO reacts with $NH_3$ on a Pt surface and this reaction has been shown to exhibit oscillatory behavior [34,35]. The possibility therefore exists that it is in fact not the reaction between NO and $H_2$ which produces kinetic oscillations, but rather the reaction between NO and the reaction product $NH_3$. Experiments which are currently underway show that oscillations do indeed occur in the NO + $NH_3$ reaction on Pt(100) in the $10^{-6}$ mbar range between 420 and 440 K [33]. Since $NH_3$ will probably only react with NO via complete dissociation into $N_{ad}$ and $H_{ad}$, the reaction sequence R3 to R5 and hence the autocatalysis provided by these steps will still be valid. The question remains, however, as to how effective $NH_3$ will be in inhibiting the surface reaction and whether intermediates $NH_x$ ($x = 1, 2$) have to be incorporated into the mechanism. If these intermediates are long-lived, their formation and decay could play the role of a slow buffer step in the oscillation mechanism. In order to determine if the NO + $NH_3$ reaction is the decisive factor in leading to oscillations in the NO + $H_2$ system, a detailed analysis of the NO + $NH_3$ reaction is in progress.

## 5. Conclusions

The reaction of NO + $H_2$ on Pt(100) has been shown to lead to the principal products of $N_2$, $NH_3$ and $H_2O$. Whereas reaction on the 1 × 1 surface yields large amounts of both $N_2$ and $NH_3$, a well-annealed hex phase has low activity. The stationary branches of the reaction exhibit a rather complex hysteresis that is associated with the $1 \times 1 \rightleftharpoons$ hex phase transition of the Pt(100) substrate. When the $1 \times 1 \rightarrow$ hex reconstruction is incomplete, i.e., when a large number of defects exist on the surface, then the overall catalytic is still high, but $NH_3$ formation is suppressed in favor of $N_2$ production. The selectivity of the reaction as given by the product ratio $NH_3/N_2$ is determined by the hydrogen adsorption rate. Accordingly, the rate of $NH_3$ formation is high when the surface is a 1 × 1 state and also when the partial pressure ratio $p_{H_2}/p_{NO}$ is high.

Kinetic oscillations in the $10^{-6}$ mbar range between 430 and 445 K have been found in the NO + $H_2$ reaction on Pt(100). The oscillations could be followed in the $N_2$ and $H_2O$ production rate and through the variations in the work function. The region of parameter space in which oscillations occur coincides with the occurrence of the hex $\rightarrow 1 \times 1$ phase transition and a decrease in the work function which reflects the onset of $NH_3$ formation. Since the temperature range in which kinetic oscillations are found is close to the temperature where "explosive" product formation occurs in TPR experiments with coadsorbed NO and $H_2$, the autocatalytic reaction step which causes the "surface explosions" is very likely to play an essential role in the oscillation mechanism.

## Acknowledgements

Financial support by the Alexander von Humboldt Stiftung (M.S.) is gratefully acknowledged. The authors would like to thank S. Wasle for the preparation of the drawings.

## References

[1] W.F. Egelhoff, Jr., in: The Chemical Physics of Solid Surfaces and Heterogeneous Catalysis, Vol. 4, Fundamental Studies of Heterogeneous Catalysis, Eds. D.A. King and D.P. Woodruff (Elsevier, Amsterdam, 1982).

[2] W. Adlhoch, H.-G. Lintz and T. Weisker, Surf. Sci. 103 (1981) 576.

[3] F. Schüth and E. Wicke, Ber. Bunsenges. Phys. Chem. 93 (1989) 191, 491.

[4] S.B. Schwartz and L.D. Schmidt, Surf. Sci. 206 (1988) 169.

[5] Th. Fink, J.P. Dath, R. Imbihl and G. Ertl, J. Chem. Phys. 95 (1991) 2109.

[6] M.W. Lesley and L.D. Schmidt, Surf. Sci. 155 (1985) 215.

[7] Th. Fink, J.-P. Dath, M.R. Bassett, R. Imbihl and G. Ertl, Surf. Sci. 245 (1991) 96.

[8] H.H. Madden and R. Imbihl, Appl. Surf. Sci. 48/49 (1991) 130.

[9] H.P. Bonzel, G. Brodén and G. Pirug, J. Catal. 53 (1978) 96.

[10] G. Pirug, H.P. Bonzel, H. Hopster and H. Ibach, J. Chem. Phys. 71 (1979) 593.

[11] R.J. Gorte, L.D. Schmidt and J.L. Gland, Surf. Sci. 109 (1981) 367.

[12] W.F. Banholzer and R.I. Masel, Surf. Sci. 137 (1984) 339.

[13] P. Gardner, M. Tüshaus, R. Martin and A.M. Bradshaw, Surf. Sci. 240 (1990) 112.

[14] K. Schwaha and E. Berthold, Surf. Sci. 66 (1977) 383.

[15] M.A. Barteau, E.I. Ho and R.J. Madix, Surf. Sci. 102 (1981) 99.

[16] P.R. Norton, J.A. Davies, D.K. Creber, C.W. Sitter and T.E. Jackman, Surf. Sci. 108 (1981) 205.

[17] B. Pennemann, K. Oster and K. Wandelt, Surf. Sci. 249 (1991) 35.

[18] G. Pirug and H.P. Bonzel, J. Catal. 50 (1977) 64.

[19] G.B. Fisher, Chem. Phys. Lett. 79 (1981) 452.

[20] J.M. Heras and L. Viscido, Appl. of Surf. Sci. 4 (1980) 238.

[21] H. Ibach and S. Lehwald, Surf. Sci. 91 (1980) 187.

[22] J.M. Gohndrone, C.W. Olsen, A.L. Backman, T.R. Gow, E. Yagasaki and R.I. Masel, J. Vac. Sci. Technol. A 7 (1989) 1986.

[23] W.F. Banholzer, Y.O. Park, K.M. Mak and R.I. Masel, Surf. Sci. 128 (1983) 176.

[24] J.L. Gland, Surf. Sci. 71 (1978) 327.

[25] R.J. Behm, P.A. Thiel, P.R. Norton and G. Ertl, J. Chem. Phys. 78 (1983) 7437; J. Chem. Phys. 78 (1983) 7448.

[26] P.R. Norton, K. Griffiths and P.E. Bindner, Surf. Sci. 138 (1984) 125.

[27] R. Imbihl, M.P. Cox and G. Ertl, J. Chem. Phys. 84 (1986) 3519.

[28] E.G. Seebauer, A.C.F. Kong and L.D. Schmidt, J. Chem. Phys. 88 (1988) 6597.

[29] J.L. Gland and E.B. Kolling, J. Catal. 68 (1981) 349.

[30] T. Yamada, J. Siera, H. Hirano, B.E. Nieuwenhuys and K. Tanaka, Vacuum 41 (1990) 115.

[31] M.Y. Smirnov, V.V. Gorodetskii and A.R. Cholach, in: Proc. Conf. Fundamental Aspects of Heterogeneous Catalysis Studied by Particle Beams, Eds. H.H. Brongersma and R.A. van Santen (Plenum, New York), in press.

[32] G. Veser and R. Imbihl, J. Chem. Phys., submitted.

[33] S.J. Lombardo, F. Esch and R. Imbihl, Surf. Sci. Lett., submitted.

[34] C.G. Takoudis and L.D. Schmidt, J. Phys. Chem. 87 (1983) 958.

[35] C.G. Takoudis and L.D. Schmidt, J. Phys. Chem. 87 (1983) 964.